Full Paper

Journal of the Brazilian Chemical Society

https://dx.doi.org/10.21577/0103-5053.20260060

J. Braz. Chem. Soc. **2026**, *37-Spe1*, e-20260060, 1-10

Dereplication of Secondary Metabolites from *Isabelcristinia aromatica* (Linderniaceae) by Untargeted Tandem Mass Spectrometry-Based Molecular Networking

Jackson R. G. S. Almeida, [*,a] ***Eluiza M. N. Afonso,*** [a] ***Elaine M. B. Nunes,*** [b] ***José A. de Siqueira Filho,*** [b] ***Gibson G. de Oliveira,*** [c] ***Fausto Carnevale-Neto*** [d] ***and Norberto P. Lopes*** [e]

[a]*Núcleo de Estudos e Pesquisas de Plantas Medicinais (NEPLAME), Universidade Federal do Vale do São Francisco, 56304-205 Petrolina-PE, Brazil*

[b]*Centro de Referência para Recuperação de Áreas Degradadas da Caatinga, Universidade Federal do Vale do São Francisco, 56300-000 Petrolina-PE, Brazil*

[c]*Centro Universitário FACOL, 56612-285 Vitória de Santo Antão-PE, Brazil*

[d]*Northwest Metabolomics Research Center, Department of Anesthesiology and Pain Medicine, University of Washington, 850 Republican Street, Seattle, WA 98109, United States*

[e]*Faculdade de Ciências Farmacêuticas de Ribeirão Preto, Universidade de São Paulo, 14040-903 Ribeirão Preto-SP, Brazil*

Isabelcristinia aromatica is a new monotypic species of a new genus recently described, and belongs to the Linderniaceae family. In order to investigate the phytochemical composition of *I. aromatica*, high-performance liquid chromatography with diode array detector and electrospray ionization mass spectrometric detection (HPLC-DAD-ESI-MS^2) analyses were conducted on crude methanolic extract and methanolic fraction obtained by partition from the dried leaves of the plant species. The putative annotation was carried out using UCSD Global Natural Products Social Molecular Networking (GNPS) and revealed the clustering of various classes of metabolites, including flavonoid glycoconjugates, phenylethanoids, and iridoid glycosides. The results showed the diversity of secondary metabolites in the species, and molecular networking could be considered a useful method for speeding the annotation of secondary metabolites in plant extracts.

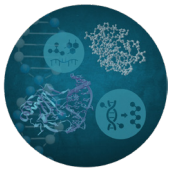

Keywords: Linderniaceae, iridoid glycosides, flavonoid glycoconjugates, phenylethanoids, GNPS

Introduction

Linderniaceae was formerly considered a synonym of Scrophulariaceae, but molecular studies have shown that some species and their close relatives do not have a unique relationship with this family. Based on this, it was proposed as a new family.[1] The family is cosmopolitan, with about 25 genera and 263 species.[2,3]

Isabelcristinia aromatica L.P. Felix & E.M. Almeida is a new monotypic species of a new genus recently described, and belongs to the Linderniaceae family, which has a pantropical distribution. In Brazil, 7 genera and 13 species occur, among which *Ameroglossum*, *Catimbaua*, and *Isabelcristinia* are considered endemic to the inselberg-type rocky outcrops in the Caatinga biome.[4]

Within the Linderniaceae family, phytochemical investigations have been conducted mainly on species of the genera *Lindernia* and *Craterostigma*. Studies on *Lindernia* species have reported the occurrence of iridoid glycosides, phenylethanoid glycosides, and flavonoids, with some extracts exhibiting antioxidant and antimicrobial activities.[5] Similarly, *Craterostigma* species are known to accumulate phenylethanoid glycosides, particularly verbascoside-type compounds, alongside caffeoyl derivatives.[6] These metabolite classes are consistent with the broader chemical profile of the order Lamiales, to which Linderniaceae belongs. The findings reported here for *I. aromatica* are discussed in light of these chemotaxonomic relationships.

*e-mail: jackson.guedes@univasf.edu.br
Editor handled this article: Paulo Wender P. Gomes (Guest)
This publication is part of the special issue "Omics Sciences"

This species is a shrub-like plant known from only six natural populations located in the municipalities of Belo Jardim, Brejo da Madre de Deus, and Jataúba, in the state of Pernambuco.[7] It is also considered endangered (EN) due to threats such as arson, overgrazing by goats and cattle, and the recreational use of inselbergs, which negatively impact its populations. Therefore, efforts to expand knowledge about the ecology and phytochemistry of *I. aromatica*, still poorly understood by science, are essential to support future research and potentially remove the species from the red list of endangered species, particularly through the recognition of its potential for the pharmaceutical industry.

The following studies reveal the valuable phytochemical potential and observations made in the field, particularly regarding the resinous odor noticeable in the leaves and branches, which are velvety due to glandular trichomes that accumulate substances. These characteristics are associated with the specific epithet of the species. To date, no medicinal use of this species has been reported by the communities visited. To the best of our knowledge, there are no studies describing the chemical composition of this species. Thus, this work is the first phytochemical study of *I. aromatica*.

Experimental

Plant material

Fresh leaves of *I. aromatica* were collected in Petrolina (coordinates: S 09°32'59.29"; W 40°55'10.44"), State of Pernambuco, Brazil. Botanical identification was performed by Elaine M. B. Nunes and José A. de Siqueira Filho by comparison with a voucher specimen (No. 6823) previously deposited at Herbário do Vale do São Francisco (HVASF) from Universidade Federal do Vale do São Francisco (UNIVASF). All procedures for access to genetic patrimony and associated traditional knowledge were carried out and the project was registered in SisGen (Register No. AAA1ACA).

Extraction

Dried and pulverized leaves (30.8 g) were initially extracted by maceration with methanol at room temperature (25 °C). Methanol was selected due to its broad solvation capacity for medium- to high-polarity secondary metabolites, including the glycosylated iridoids, phenylethanoids, and flavonoids characteristic of Lamiales species. The extracted solution was concentrated in a rotatory evaporator to obtain the crude methanolic extract (13.54 g). The extract (10 g) was submitted to solubilization in 100 mL of methanol and subsequently partitioned with hexane to obtain the hexane (0.3 g) and methanolic (9 g) fractions. The hexane fraction was not included in the metabolomics workflow, as the study focused on the polar metabolite pool; non-polar constituents will be addressed in future work.

Metabolomics analysis

Samples were prepared and analyzed as previously described.[8-10] The extract and fraction (ca. 2.0 mg) were dissolved in MeOH/H_2O (1.0 mL, 1:1, v/v) and submitted to solid phase extraction (SPE) for the removal of non-polar constituents. We used C_{18} cartridges SPE cartridge (Strata C18-E, 100 mg mL^{-1}, Phenomenex) activated with 5.0 mL of MeOH and equilibrated with 5.0 mL of MeOH/H_2O (1:1, v/v). The resulted samples were dried under N_2 atmosphere and dissolved at final concentration 2 mg mL^{-1}, filtered through a 0.45 µm GHP Acrodisk (Millipore), and injected into the high-performance liquid chromatography (HPLC).

High performance liquid chromatography ultraviolet tandem mass spectrometry (HPLC-UV-MS^2) experiments were performed using an UFLC (Shimadzu) system with two LC20AD solvent pumps, a $SIL20A_{HT}$ auto sampler, a CTO20A column oven and a CBM20A controller, coupled with an Ion Trap Mass Spectrometer (AmaZon SL). Each sample was injected at 20 µL for analysis in both positive and negative electrospray ionization (ESI) modes. The chromatographic separation was performed on a C_{18} column (Phenomenex, 250 mm × 4.6 mm × 5 µm) using the following gradient elution: solvent A = H_2O and acetic acid (0.1% v/v); solvent B = ACN and formic acid (0.1% v/v); elution profile = 0.0-30.0 min (10-100% B); 30.0-40.0 min (100% B); 40.0-45.0 min (100-10% B); 45.0-60.0 min (10% B), column oven at 35 °C, and flow rate of 1.0 mL min^{-1}. The UV spectra were set to record absorption at λ 200-800 nm. MS and MS^2 acquisition parameters were as follows: capillary 3.5 kV, positive and negative ESI modes, end plate offset 500 V, nebulizer 40 psi, dry gas (N_2) with flow of 8 L min^{-1} and temperature of 300 ºC. Collision-induced dissociation (CID) fragmentation experiments were carried out in data-dependent acquisition (DDA) mode, selecting 2 precursor ions *per* cycle, and CID amplitude 75%. MS and MS^2 scan range of *m/z* 100-1200.

Molecular networking

Data were converted to mzXML format directly from Bruker DataAnalysis 4.2 (Bruker Daltonik GmbH, Bremen, Germany). The files were uploaded to the UCSD Global Natural Products Social Molecular Networking (GNPS)[11,12] FTP-server[13] and subjected to METBOLOMICS-SNETS

workflow with the following parameters: parent mass tolerance 2.0 Da, ion tolerance 0.5 Da, minimal pair cosine 0.5, network topK 10, maximum connected component size 100, minimum matched peaks 6, minimum cluster size 2. Metabolites were putatively annotated by searching the GNPS database using a score above 0.8 and at least 2 matched peaks. Data were visualized via Cytoscape (version 3.2.1, Institute of Systems Biology, Seattle, USA).[14] The networks were arranged as Cytoscape's organic layout, node colors were mapped based on the source of the MS^2 data and the edge thickness attribute was defined to reflect cosine similarity scores, with thicker lines representing higher similarity. To avoid misinterpretation of LC-contaminants and/or noise, blank injections (mobile phase) were input to Spectral Networks. All networks can be accessed online (links provided in the Supplementary Information (SI) section).

Compound annotations were assigned following the Metabolomics Standards Initiative (MSI) reporting standards. Compounds matched to the GNPS spectral library (cosine score ≥ 0.8, ≥ 2 matched peaks) or manually annotated by comparison of MS^2 fragmentation patterns and UV spectra with published literature data were assigned as MSI level 2 (putatively annotated compounds). No compound isolation or analysis with authentic reference standards was performed in this study; therefore, no MSI level 1 annotations are reported.

Results and Discussion

In order to investigate the phytochemical composition of *I. aromatica*, HPLC-DAD-ESI-MS^2 analyses were conducted on crude methanolic extract and methanolic fraction obtained from liquid-liquid partition of the dried leaves, resulting in more than 14,000 MS^2 spectra. The base-peak chromatograms are depicted in Figures 1 and 2. It should be noted that both samples represent the polar metabolite pool, as the extraction and sample preparation steps consistently targeted medium- to high-polarity compounds; non-polar constituents are therefore not represented in the present dataset.

GNPS merged the MS^2 spectra into 750 nodes (288 for ESI^+ and 462 for ESI^-) using MSCluster algorithm.[8-15] Molecular networking (MN) was created for each ionization mode. After blank removal, the MNs consisted of 262 nodes (99 for ESI^+ and 163 for ESI^-). The nodes were grouped according to cosine similarity scoring and putatively annotated based on GNPS automated library searching.[11] We manually inspected the candidate hits to match UV spectra and explore the gas-phase fragmentation reactions.[16] The putative annotation, conducted at MSI level 2 (putatively annotated compounds and putatively characterized compound classes, respectively), revealed the clustering of various classes of metabolites, including flavonoid glycoconjugates, phenylethanoids, and iridoid glycosides, as shown in Figures 3a-3b. Chromatographic and spectral properties of detected compounds are given in Table 1.

Two clusters formed in the ESI^+ MN were characterized by the neutral loss of 162 u (Figure 4) or sequential eliminations of 162 and 176 u (Figure S1, SI section). Such mass differences are indicative of heterolytic cleavages

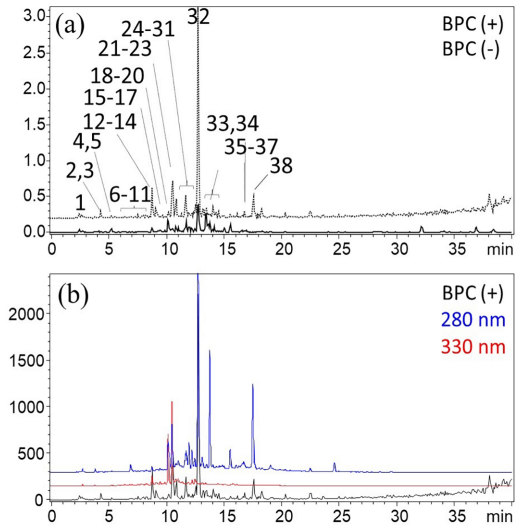

Figure 1. Representative HPLC-DAD-MS chromatogram of methanolic extract of *I. aromatica* (a) at ESI positive (dot line) and negative (continuous line) modes and (b) the comparison between base peak chromatogram (BPC) in ESI^+ and at λ 280 nm (blue line) and λ 330 nm (red line).

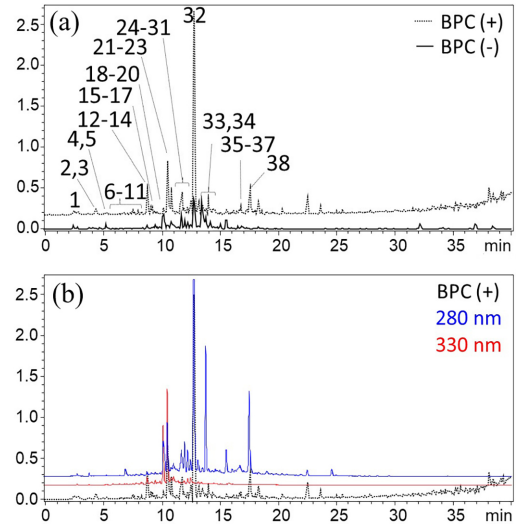

Figure 2. Representative HPLC-DAD-MS chromatogram of methanolic fraction of *I. aromatica* (a) at ESI positive (dot line) and negative (continuous line) modes and (b) the comparison between base peak chromatogram (BPC) in ESI^+ and at λ 280 nm (blue line) and λ 330 nm (red line).

of O–C bonds from glycosylated compounds containing hexosyl (162 u) and glucuronyl (176 u) substituents. Neutral losses of one or more saccharides can be generated directly at the interface of ESI source due to the lower energy bonds of *O*-glycoconjugates. The in-source fragmentation leads to formation of the Y_0^- or Y_0^+ and allows further CID-MS^2 analysis for aglycone assignment.[11-16,26,27] Manual inspection of the most intense LC peaks that constitute these MN clusters evidenced the selection of Y_0^+ as precursor ions for CID experiments. The resulting fragments *m/z* 153, 135, and 119 were previously annotated as ^{0,3}A+ and ^{0,3}B+ ions of luteolin and apigenin, possibly formed by retro-Diels Alder reactions.[2,10] UV spectra with λ_{max} 270-330 nm supported the annotation of flavones.[26]

Another MN cluster in the ESI^+ also showed recurrent neutral loss of 162 u and the fragment *m/z* 163 (Figure S2, SI section). Since the MS^2 spectra were acquired on a low-resolution instrument and we employed a fragment ion tolerance of 0.2 Da to generate the MNs, the loss of 162 u can represent the elimination of hexosyl or caffeoyl residues, which are isobaric at unit mass resolution and thus cannot be distinguished solely on the basis of nominal mass. Manual examination showed that these compounds eluted at 6.6-7.5 min, which suggests higher polarity, and absorbed at λ_{max} 297 and 324 nm, an indicative of caffeoylquinic acids.[28] MS^2 spectra supported the annotation by revealing that the fragment related to 162 u elimination were at very low signal intensity (< 10%), not expected to *O*-glycosides at similar experimental conditions, and the product ion *m/z* 163 which suggest the presence of an anhydro-caffeoyl moiety, as previously observed.[28]

Along with flavone glycoconjugates and caffeoyl derivatives, iridoids and phenylethanoids were putatively annotated in the ESI^- MN. Iridoids represent a large group of monoterpenoids formed by a cyclopentanopyran nucleus, generally found in plants stabilized by esterification or glycosylation.[29] The preferential formation of formate adducts $[M + HCOO]^-$ in negative mode - in the presence of formic acid in the mobile phase - is a well-established diagnostic indicator of iridoids bearing a C-4 methyl ester or lactone functionality, as described for compounds such as catalpol, loganin, and gardoside.[30] Here, iridoids were distributed across different clusters of the MN due to their chemical variability. In one small group (Figure 5), the nodes comprised formate adducts $[M + HCOO]^-$ sharing the same neutral loss of hexose (162 u), consistent with *O*-glucosylation. After glycosidic bond cleavage, the resulting aglycone ions underwent sequential neutral losses of 18 u (dehydration) and 28 u (CO elimination), generating a series of ring-opening fragments characteristic of the cyclopentanopyran iridoid scaffold.[30] Additionally, UV absorption at λ ca. 200-240 nm, with no significant absorption above 300 nm, was consistent with the absence of extended conjugation, further distinguishing these nodes from flavonoid and phenylethanoid clusters. The compounds were putatively annotated as methyl-catalpol (3), angeloside (4), and bartsioside (38) by comparison of their precursor masses,

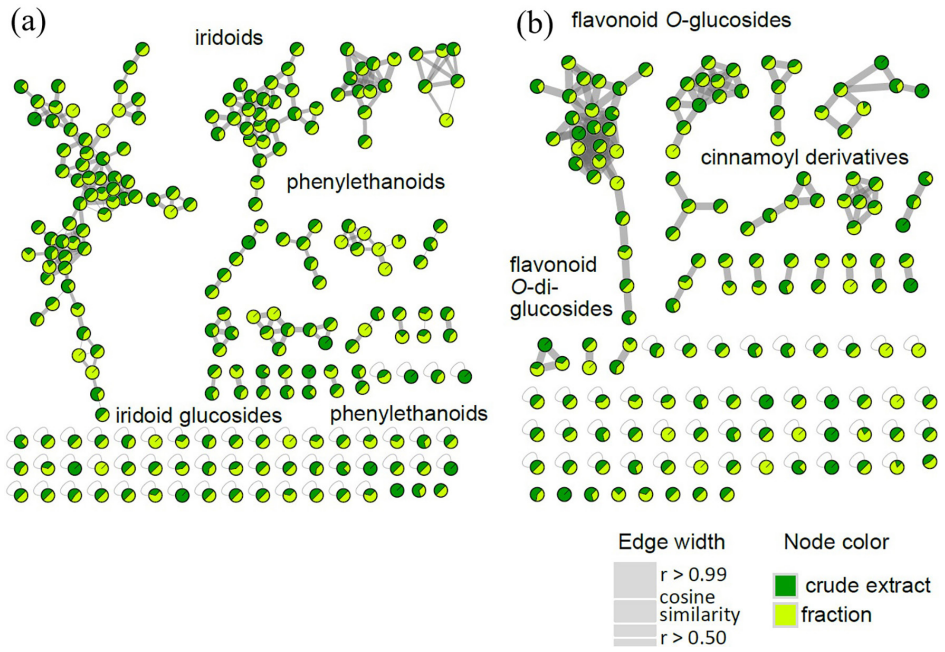

Figure 3. Representation of molecular networking application based on LC-MS^2 (a) negative ESI and (b) positive ESI ionization modes, after blank removal showing the clusters related to flavonoid-*O*-glucosides and iridoids. Node text indicates the parent ion, node color chart reflects the extract and edge width depicts cosine similarity (the larger the similarity degree, the larger edge width).

Table 1. Metabolites from *I. aromatica* annotated by HPLC-DAD-MS^2

No.	t_R / min	UV max / nm	Annotation[a]	$[M - H]^-$	Fragmentation	$[M + H]^+$	Fragmentation	Matrix	Reference
1	2.9-3.0	200	catalpol	407.2	MS^2[407] 361; 199; 169	–	–	E, F	17
2	3.9-4.0	280	catalpol isomer	407.3	MS^2[407] 361; 199; 169	–	–	E, F	17
3	4.0-4.2	230	methyl-catalpol	421.1[a]	MS^2[421] 375; 195; 179	–	–	E, F	18
4	4.8-4.9	209	angeloside	393.2[a]	MS^2[393] 347; 329; 185; 167; 149	–	–	E, F	19
5	5.4-5.5	235	decaffeoyl-verbascoside	461.1	MS^2[461] 377; 315; 297; 161; 135	485.2	MS^2[485] 425; 331; 273; 177	F	17
6	6.3-6.4	285,330(sh)	dicaffeoylquinic acid	499.1	MS^2[499] 355; 163	–	–	E, F	20
7	7.2-7.3	287,327(sh)	caffeoyl-*O*-coumaroylquinic acid	483.1	MS^2[483] 479; 355; 163	–	–	E, F	20
8	7.5-7.7	286, 330	apigenin-di-*C*-hexoside	593.1	MS^2[593] 575; 557; 503; 473; 353	595.2	MS^2[595] 577; 559; 541; 529; 511; 475; 457; 409; 355; 309	E, F	17
9	8.0-8.1	210, 313	verminoside	523.2	MS^2[523] 323; 221; 179	–	–	E, F	17
10	8.2-8.3	213, 305	verminoside isomer	523.1	MS^2[523] 323; 221; 179	–	–	E, F	17
11	8.4-8.5	223, 313	hydroxy-verbascoside	639.2	MS^2[639] 621; 487; 469; 459; 179	–	–	E, F	17
12	8.8-8.9	267(sh), 340	luteolin-*O*-hexosyl-glucuronide	623.1	MS^2[623] 447; 285	625.2	MS^2[625] 449; 431; 287	E	16,21
13	9.0-9.2	297, 330	pentahydroxyflavone-*O*-hexoside	463.1	MS^2[463] 301	465.2	MS^2[465] 303	E, F	16,21
14	9.1-9.2	213, 310	specioside	507.2	MS^2[507] 345; 307; 163	–	–	E, F	17
15	9.5-9.6	293, 325	hydroxy-globularinin	–	–	529.1	MS^2[529] 493; 349; 331; 313; 295; 183; 165	E, F	17
16	9.5-9.6	283.331	alpinoside	461.2	MS^2[461] 415 MS^2[461→415] 355; 311; 233; 191; 149	–	–	F	17
17	9.7-9.8	288	aucubin	391.2	MS^2[391] 345; 255; 207; 183; 139	–	–	E, F	17
18	10.2-10.3	288, 330	luteolin-*O*-hexosyl-deoxyhexoside	–	–	595.2	MS^2[595] 449; 287	E, F	16,21
19	10.3-10.4	289, 330	verbascoside	623.2	MS^2[623] 461	–	–	E	17
20	10.3-10.6	282	globularinin	555.2[a]	MS^2[555] 509; 361; 199	–	–	E, F	17
21	10.6-10.8	254, 267(sh), 347	luteolin-*O*-hexoside	447.1	MS^2[447] 285	449.1	MS^2[449] 287; 149	E, F	16,21
22	10.8-10.9	271, 335(sh)	luteolin-*O*-hexosyl-glucuronide	623.1	MS^2[623] 461; 285 MS^2[623→461] 285	625.2	MS^2[625→463] 287	E	16,21
23	10.9-11.0	286, 330(sh)	globularimin	509.2	MS^2[509] 465; 347; 329; 221; 180	511.2	MS^2[511] 493; 457; 349; 331; 311; 303; 293; 283; 267; 249; 231; 211; 183; 167; 165; 163; 149; 147	E, F	17
24	11.0-11.1	286, 329	nemoroside	573.2	MS^2[5573] 527; 361; 347; 343; 199;184	–	–	E, F	22
25	11.0-11.1	286, 326	verbascoside isomer	623.2	MS^2[623] 509; 461	–	–	E	17
26	11.4-11.7	281	leucosceptoside A	637.3	MS^2[637] 461; 443; 299; 265; 193	639.3	MS^2[639] 493; 459; 331; 313; 287;	E, F	17
27	11.6-11.7	285, 330	nemorososide	559.2	MS^2[559] 513; 347; 185	–	–	E, F	22

Table 1. Metabolites from *I. aromatica* annotated by HPLC-DAD-MS^2 (cont.)

No.	t_R / min	UV max / nm	Annotation[a]	$[M - H]^-$	Fragmentation	$[M + H]^+$	Fragmentation	Matrix	Reference
28	11.8-11.9	277	globularin	537.2[a]	MS^2[537] 491	493.2	MS^2[493] 331; 313; 295; 277; 183; 165; 149; 131 MS^2[493→331] 313; 183; 165; 149; 131	E, F	21,23
29	12.0-12.1	280, 340(sh)	trihydroxyflavanone-*O*-hexoside	–	–	433.1	MS^2[433] 271	E, F	21,23
30	12.2-12.5	281, 330(sh)	methoxy-luteolin-*O*-hexoside	–	–	463.1	MS^2[463] 301; 287	E, F	–
31	12.6-12.7	281, 330(sh)	luteolin-*O*-hexoside	447.2	MS^2[447] 285; 261; 242; 167	449.1	MS^2[449] 287; 181; 153	E, F	21,23
32	12.8-13.0	267, 293	globularin isomer	537.2[a]	MS^2[537] 491	493.2	MS^2[493] 331; 313; 295; 277; 183; 165; 149; 131 MS^2[493→331] 313; 183; 165; 149; 131	E, F	21,23
33	13.4-13.6	280	nemorososide isomer	559.2[a]	MS^2[559] 513; 345; 329; 183; 149	–	–	E, F	–
34	14.0-14.2	280	unknown	563.2	MS^2[563] 529; 351	–	–	E, F	–
35	14.5-14.7	281, 335(sh)	luteolin-*O*-hexosyl-deoxyhexoside	593.1	MS^2[593] 285	595.1	MS^2[595] 287	E, F	16,21
36	16.6-16.9	279	asperuloside	459.3[a]	MS^2[459] 413; 251	–	–	F	17
37	16.7-16.8	279	bellidifolin-*O*-hexoside	–	–	437.2	MS^2[437] 275; 257; 231	E, F	24
38	17.4-17.7	276	bartsioside	375.2[a]	MS^2[375] 329; 311; 285; 265; 249; 181; 163	–	–	E, F	25

[a]$[M - H - HCOOH]^-$ annotation confidence levels assigned according to the Metabolomics Standards Initiative (MSI) reporting standards: level 2, putatively annotated based on GNPS spectral library match (cosine score ≥ 0.8) or MS²/UV comparison with literature. sh: shoulder; E: extract; F: fraction.

fragmentation patterns, and UV profiles with literature data.

Glycosylated forms of iridoids and phenylethanoids were progressively grouped in distinct regions of the same cluster, driving by the distribution of structurally related molecules according to their MS^2 fragmentation patterns (Figure 6). The nodes related to phenylethanoids showed a loss of 162 u (caffeic acid) followed by another loss of 146 u, attributed to a deoxyhexosyl substituent. Their annotation as leucosceptoside A (26) and verbascoside (19,25) were supported by comparison of UV and MS^2 spectra from literature.[17] One node within the same cluster yielded major loss of 146 u, followed by loss of 180 u, and was annotated as decaffeoylverbascoside (5).[17] We observed another region of the MN with nodes that share the fragment *m/z* 179, indicating the elimination of one caffeoyl residue. Comparison with UV and MS^2 spectra suggested the presence of the cinnamoyl-iridoids verminoside (9,10) and specioside (14).[17]

Another cluster propagated nodes that showed mass differences of 46 u, indicative of formate adducts $[M + HCOO]^-$ formed with formic acid from the mobile phase (Figure 7). This adduct formation is particularly characteristic of iridoid glucosides bearing a C-4 lactone or methyl ester group, such as aucubin and catalpol, which have been shown to preferentially ionize as $[M + HCOO]^-$ rather than $[M - H]^-$ under negative ESI conditions with formate-containing mobile phases.[30] These nodes diverged within the spectral network in areas populated by distinct fragmentation patterns. One region showed the neutral loss of the hexose moiety (162 u), yielding aglycone ions at *m/z* 183 and 165 for aucubin (17; $[M + HCOO - H - 162]^- = 183$, $[M + HCOO - H - 162 - 18]^- = 165$) and *m/z* 199 and 181 for catalpol (1), consistent with sequential dehydrations from the bicyclic iridoid aglycone reported in the literature.[30] The fragment at *m/z* 121 (loss of CH_2O from the dehydrated aglycone) further supported the presence of a C-11 hydroxymethyl group, a structural feature of the aucubin-type iridoids.[30] In a different area of the same cluster, we observed the loss of 166 u, attributable to the elimination of one foliamentic acid substitution, leading to tentative annotation as nemoroside (24) and nemorososide (27).[22] These nodes shared UV absorption in the range of λ 275-290 nm, consistent with a *p*-hydroxyphenyl chromophore present in foliamentoyl-iridoids. Globularimin (23) was also detected, displaying UV absorbance and a fragmentation pattern comparable to those previously described for *Globularia* spp.[17]

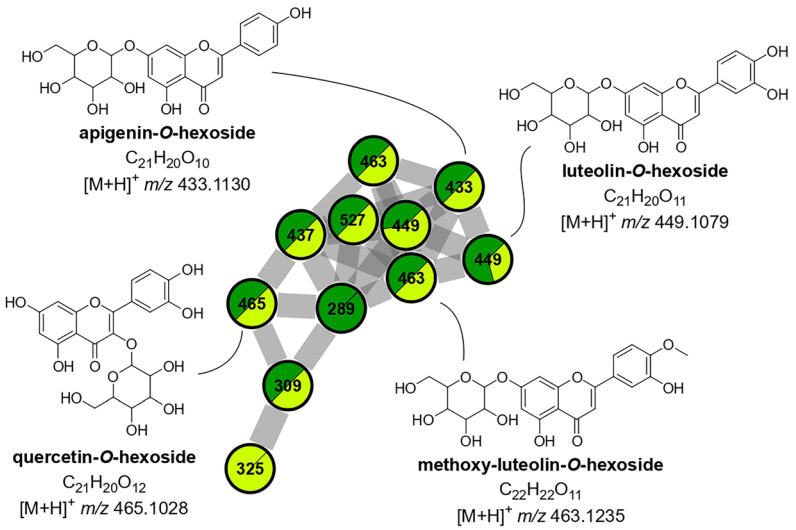

Figure 4. MN applied to LC-(+)-ESI-MS^2 data showing flavone glycoconjugates. Node label represents the precursor mass (*m/z*).

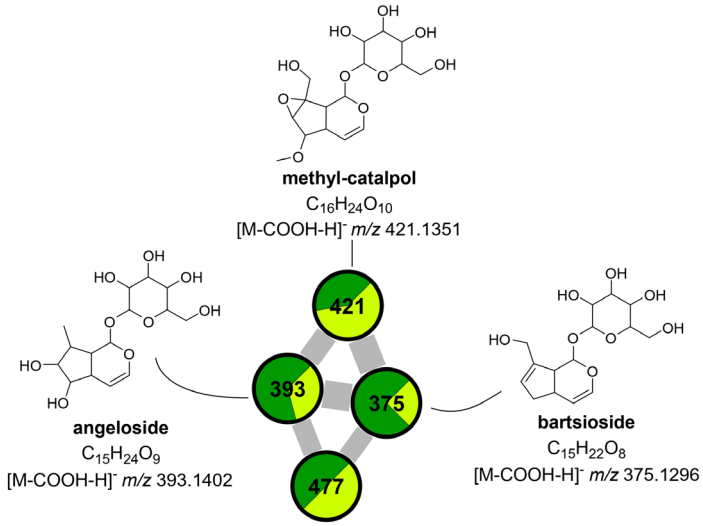

Figure 5. MN applied to LC-(−)-ESI-MS^2 data showing iridoid glycosides.

In positive ion mode, CID-MS^2 of globularin (28) resulted in the protonated molecule $[M + H]^+$ *m/z* 493 and led to cleavages of the glycosidic substituent ($[M - 162 + H]^+ = 331$ for precursor ion), followed by elimination of the cinnamoyl moiety ($[M - 162 - 148 + H]^+$ *m/z* 183), and dehydrations from the iridoid scaffold (leading to *m/z* 313, 295, 165 and 147, as showed in Figure S3, SI section).

Conclusions

In the present study, the polar chemical composition of the leaves of *I. aromatica* was described for the first time using HPLC-DAD-ESI-MS^2 and molecular networking. The results revealed a diversity of medium- to high-polarity secondary metabolites, particularly iridoid glycosides, phenylethanoid glycosides, and flavonoid glycoconjugates, and demonstrate that molecular networking is a powerful tool for accelerating the annotation of secondary metabolites in plant extracts. The use of methanol as the extraction solvent and C18-SPE sample cleanup consistently targeted this polar metabolite pool; however, these choices inherently limit coverage of non-polar chemical classes. Future studies employing complementary extraction strategies and, ideally, compound isolation and NMR-based structural confirmation, will be essential to provide a comprehensive view of the total metabolome of this endangered and chemotaxonomically novel species.

Supplementary Information

Supplementary information (Figures S1 to S41) is available free of charge at http://jbcs.sbq.org.br as PDF.

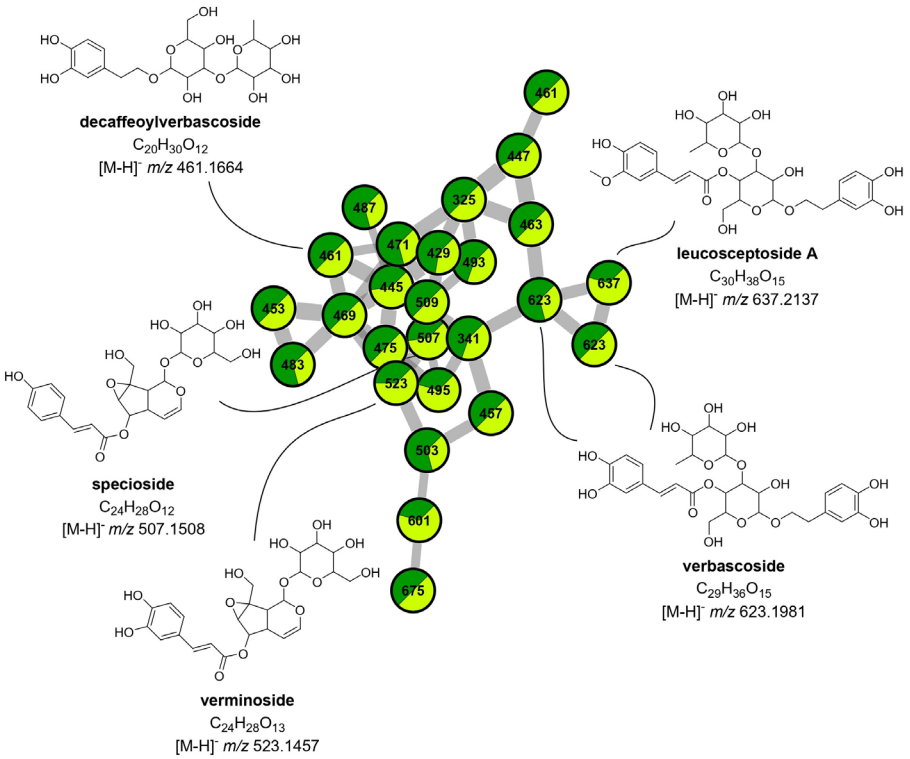

Figure 6. MN applied to LC-(−)-ESI-MS^2 data showing iridoid glycosides and phenylethanoids.

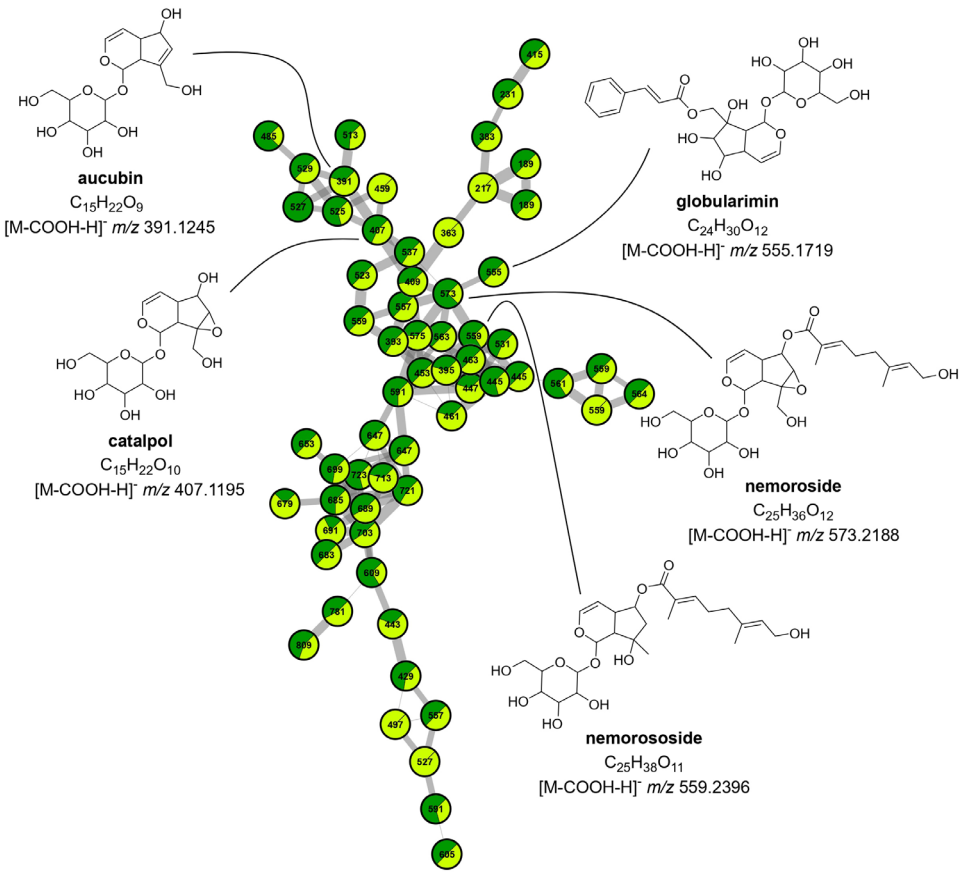

Figure 7. MN applied to LC-(−)-ESI-MS^2 data showing esterified glycosylated iridoids.

Data Availability Statement

The default parameters of the molecular networks can be access at: [Link] and [Link]

Acknowledgments

The authors thank to Brazilian agencies CNPq and FAPESP for the financial support.

Author Contributions

Conceptualization: J.R.G.S.A. and F.C.N.; plant collection and botanical identification: E.M.B.N. and J.A.S.F.; methodology: J.R.G.S.A., F.C.N. and G.G.O.; data curation: J.R.G.S.A., E.M.N.A., N.P.L. and F.C.N.; writing-original draft preparation: J.R.G.S.A., E.M.N.A. and F.C.N.; writing-review and editing: J.R.G.S.A., E.M.N.A., N.P.L. and F.C.N. All authors have read and agreed to the published version of the manuscript.

References

1. Rahmanzadeh, R.; Müller K.; Fischer E.; Bartels, D.; Borsch, T.; *Plant Biol.* **2005**, *7*, 67. [Crossref]
2. Fischer, E.; Vogel, S.; Lopes, A. V.; *Feddes Repertorium* **1999**, *110*, 529. [Crossref]
3. Christenhusz, M. J.; Byng, J. W.; *Phytotaxa* **2016**, *261*, 201. [Crossref]
4. Souza, V. C.; Lorenzi, H.; *Botânica Sistemática: Guia Ilustrado para Identificação das Famílias de Fanerógamas Nativas e Exóticas no Brasil, Baseado em APG IV'*, 4th ed.; Nova Odessa: Jardim Botânico Plantarum, 2019.
5. Tsai, Y. C.; Hohmann, J.; El-Shazly, M.; Chang, L. K.; Dankó, B.; Kúsz, N.; Hsieh, C. T.; Hunyadi, A.; Chang, F. R.; *J. Ethnopharmacol*. **2020**, *250*, 25. [Crossref]
6. Passon, M.; Weber, F.; Jung, N. U.; Bartels, D.; *Phytochem. Anal*. **2021**, *32*, 4. [Crossref]
7. Almeida, E. M.; Wanderley, A. M.; Santos, A. S.; Melo, J. I. M.; Souza, G.; Batista, F. R. C.; Christenhusz, M. J. M.; Felix, L. P.; *Phytotaxa* **2019**, *400*, 215. [Crossref]
8. Castro-Gamboa, I.; Burgos, R.; Cardoso, P.; Carnevale, F.; Pilon, A.; Lopes, M. N.; Silva, D.; Bolzani, V.; *Planta Med.* **2010**, *76*, 1188. [Crossref]
9. Pilon, A. C.; Gu, H.; Raftery, D.; Bolzani, V. S.; Lopes, N. P.; Castro-Gamboa, I.; Carnevale Neto, F.; *Anal. Chem.* **2019**, *91*, 10413. [Crossref]
10. Carnevale Neto, F.; Siquitelli, C. D.; Pilon, A. C.; Silva, D. H. S.; Bolzani, V. S.; Castro-Gamboa, I.; *J. Braz. Chem. Soc.* **2013**, *24*, 758. [Crossref]
11. Wang, M.; Carver, J. J.; Phelan, V. V.; Sanchez, L. M.; Garg, N.; Peng, Y.; Nguyen, D. D.; Watrous, J.; Kapono, C.A.; Luzzatto-Knaan, T.; Porto, C.; Bouslimani, A.; Melnik, A. V.; Meehan, M. J.; Liu, W.; Crüsemann, M.; Boudreau, P. D.; Esquenazi, E.; Sandoval-Calderón, M.; Kersten, R. D.; Pace, L. A.; Quinn, R. A.; Duncan, K. R.; Hsu, C.; Floros, D. J.; Gavilan, R. G.; Kleigrewe, K.; Northen, T.; Dutton, R. J.; Parrot, D.; Carlson, E. E.; Aigle, B.; Michelsen, C. F.; Jelsbak, L.; Sohlenkamp, C.; Pevzner, P.; Edlund, A.; McLean, J.; Piel, J.; Murphy, B. T.; Gerwick, L.; Liaw, C.; Yang, Y.; Humpf, H.; Maansson, M.; Keyzers, R. A.; Sims, A. C.; Johnson, A. R.; Sidebottom, A. M.; Sedio, B. E.; Klitgaard, A.; Larson, C. B.; Boya, C. A.; Torres-Mendoza, D.; Gonzalez, D. J.; Silva, D. B.; Marques, L. M.; Demarque, D. P.; Pociute, E.; O'Neill, E. C.; Briand, E.; Helfrich, E. J. N.; Granatosky, E. A.; Glukhov, E.; Ryffel, F.; Houson, H.; Mohimani, H.; Kharbush, J. J.; Zeng, Y.; Vorholt, J. A.; Kurita, K. L.; Charusanti, P.; McPhail, K. L.; Nielsen, K. F.; Vuong, L.; Elfeki, M.; Traxler, M. F.; Engene, N.; Koyama, N.; Vining, O. B.; Baric, R.; Silva, R. R.; Mascuch, S. J.; Tomasi, S.; Jenkins, S.; Macherla, V.; Hoffman, T.; Agarwal, V.; Williams, P. G.; Dai, J.; Neupane, R.; Gurr, J.; Rodríguez, A. M. C.; Lamsa, A.; Zhang, C.; Dorrestein, K.; Duggan, B. M.; Almaliti, J.; Allard, P.; Phapale, P.; Nothias, L.; Alexandrov, T.; Litaudon, M.; Wolfender, J.; Kyle, J. E.; Metz, T. O.; Peryea, T.; Nguyen, D.; VanLeer, D.; Shinn, P.; Jadhav, A.; Müller, R.; Waters, K. M.; Shi, W.; Liu, X.; Zhang, L.; Knight, R.; Jensen, P. R.; Palsson, B. O.; Pogliano, K.; Linington, R. G.; Gutiérrez, M.; Lopes, N. P.; Gerwick, W. H.; Moore, B. S.; Dorrestein, P. C.; Bandeira, N.; *Nat. Biotechnol.* **2016**, *34*, 828. [Crossref]
12. Watrous, J.; Roach, P.; Alexandrov, T.; Heath, B. S.; Yang, J. Y.; Kersten, R. D.; Voort, M.; Pogliano, K.; Gross, H.; Raaijmakers, J. M.; Moore, B. S.; Laskin, J.; Bandeira, N.; Dorrestein, P. C.; *Proc. Natl. Acad. Sci. U.S.A.* **2012**, *109*, E1743. [Crossref]
13. GNPS. [Link] accessed in March 2026
14. Shannon, P.; Markiel, A.; Ozier, O.; Baliga, N. S.; Wang, J. T.; Ramage, D.; Amin, N.; Schwikowski, B.; Ideker, T.; *Genome Res*. **2003**, *13*, 2498. [Crossref]
15. Frank, A. M.; Bandeira, N.; Shen, Z.; Tanner, S.; Briggs, S. P.; Smith, R. D.; Pevzner, P. A.; *J. Proteome Res*. **2008**, *7*, 113. [Crossref]
16. Demarque, D. P.; Crotti, A. E. M.; Vessecchi, R.; Lopes, J. L. C.; Lopes, N. P.; *Nat. Prod. Rep*. **2016**, *33*, 432. [Crossref]
17. Friščić, M.; Bucar, F.; Pilepić, K. H.; *J. Mass Spectrom*. **2016**, *51*, 1211. [Crossref]
18. Nie, R.; Zhang, Y.; Jin, Q.; Zhang, S.; Wu, G.; Chen, L.; Zhang, H.; Wang, X.; *Food Res. Int*. **2021**, *139*, 109916. [Crossref]
19. Gómez-Caravaca, A. M.; Segura-Carretero, A.; Fernández-Gutiérrez, A.; Caboni, M. F.; *J. Agric. Food Chem.* **2011**, *59*, 10815. [Crossref]
20. Asamenew, G.; Kim, H. W.; Lee, M. K.; Lee, S. H.; Lee, S.; Cha, Y. S.; Lee, S. H.; Yoo, S. M.; Kim, J. B.; *Food Chem: X* **2019**, *2*, 100033. [Crossref]

21. Qin, Y.; Gao, B.; Shi, H.; Cao, J.; Yin, C.; Lu, W.; Yu, L.; Cheng, Z.; *J. Pharm. Biomed. Anal*. **2017**, *142*, 113. [Crossref]
22. Junior, P.; *Planta Med*. **1983**, *47*, 67. [Crossref]
23. Es-Safi, N.; Kerhoas, L.; Ducrot, P. H.; *Spectrosc. Lett*. **2007**, *40*, 695. [Crossref]
24. Wolfender, J.; Maillard, M.; Marston, A.; Hostettmann, K.; *Phytochem. Anal*. **1992**, *3*, 193. [Crossref]
25. Kumar, V.; Sood, H.; Sharma, M.; Chauhan, R. S.; *Phytochem. Anal*. **2013**, *24*, 598. [Crossref]
26. de Oliveira, G. G.; Neto, F. C.; Demarque, D. P.; Pereira-Junior, J. A. S.; Peixoto Filho, R. C. S.; de Melo, S. J.; Almeida, J. R. G. S.; Lopes, J. L. C.; Lopes, N. P.; *Planta Med*. **2016**, *83*, 636. [Crossref]
27. Stobiecki, M.; Kachlicki, P.; Wojakowska, A.; Marczak, Ł.; *Phytochem Lett.* **2015**, *11*, 358. [Crossref]
28. Rivera-Mondragón, A.; Tuenter, E.; Ortiz, O.; Sakavitsi, M. E.; Nikou, T.; Halabalaki, M.; Caballero-George, C.; Apers, S.; Pieters, L.; Foubert, K.; *Phytochemistry* **2020**, *177*, 112438. [Crossref]
29. Ludwiczuk, A.; Skalicka-Woźniak, K.; Georgiev, M. I. In *Pharmacognosy: Fundamentals, Applications and Strategies*; Badal, S.; Delgoda, R., eds.; Elsevier: Boston, MA, USA, 2017, ch. 11. [Link] accessed in March 2026
30. Li, C.; Zhang, X.; Xue, X.; Zhang, F.; Xu, Q.; Liang, X.; *Rapid Commun. Mass Spectrom*. **2008**, *22*, 12. [Crossref]

Submitted: December 15, 2025
Final version online: April 1, 2026